Efficient monomolecular white emission of phenothiazine boronic ester derivatives with room temperature phosphorescence

Faizal Khan[a], Lesia Volyniuk,[b] Melika Ghasemi,[b] Dmytro Volyniuk,[b] Juozas Vidas Grazulevicius[b], Rajneesh Misra[a]*

Supporting Information

Contents **Page**

Experimental Section

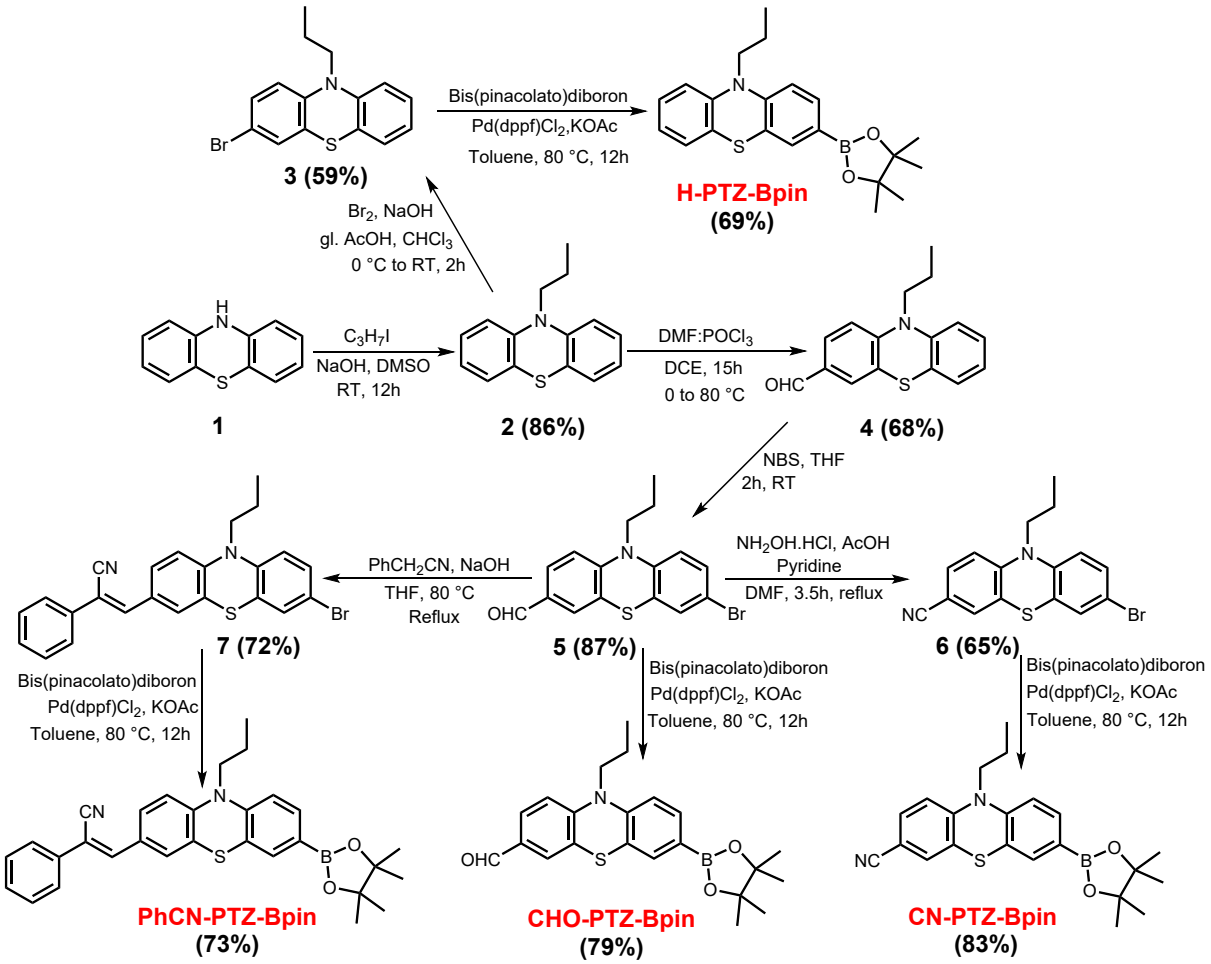

Scheme S1. Synthesis of phenothiazine derivatives **H-PTZ-Bpin**, **CHO-PTZ-Bpin**, **CN-PTZ-Bpin**, and **PhCN-PTZ-Bpin**.

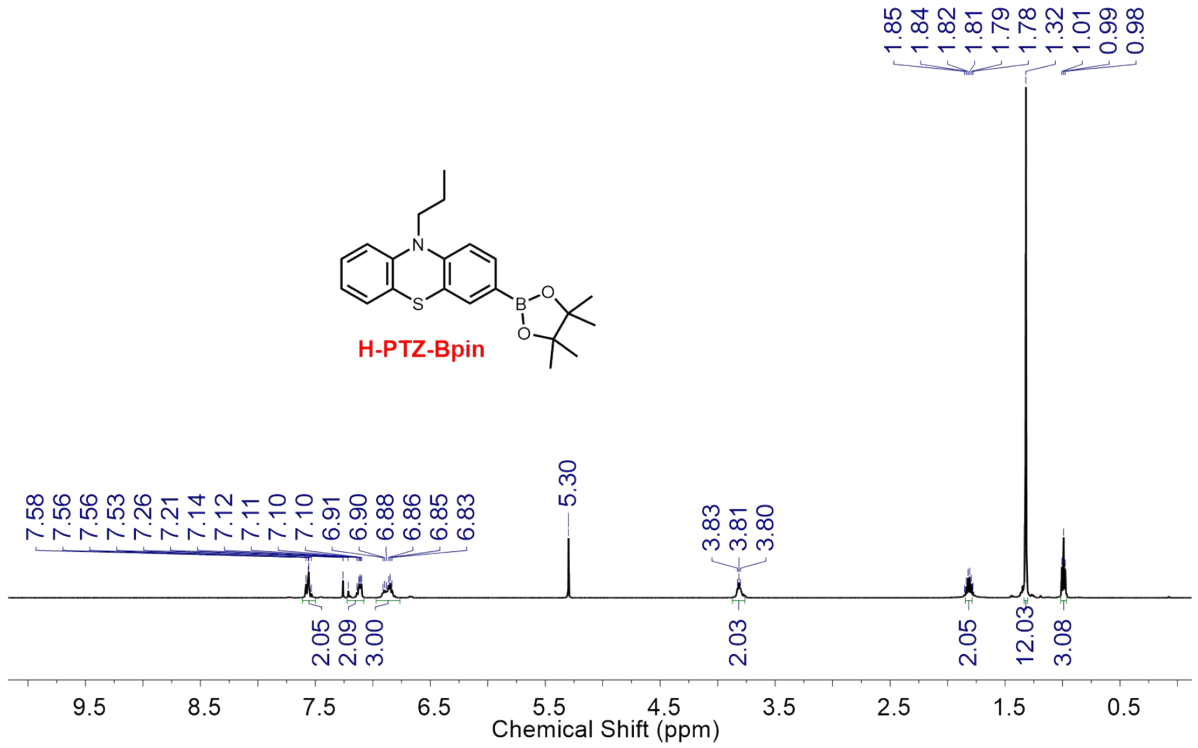

Figure S1. ^{1}H NMR of **H-PTZ-Bpin** ($CDCl_3$, 500 MHz).

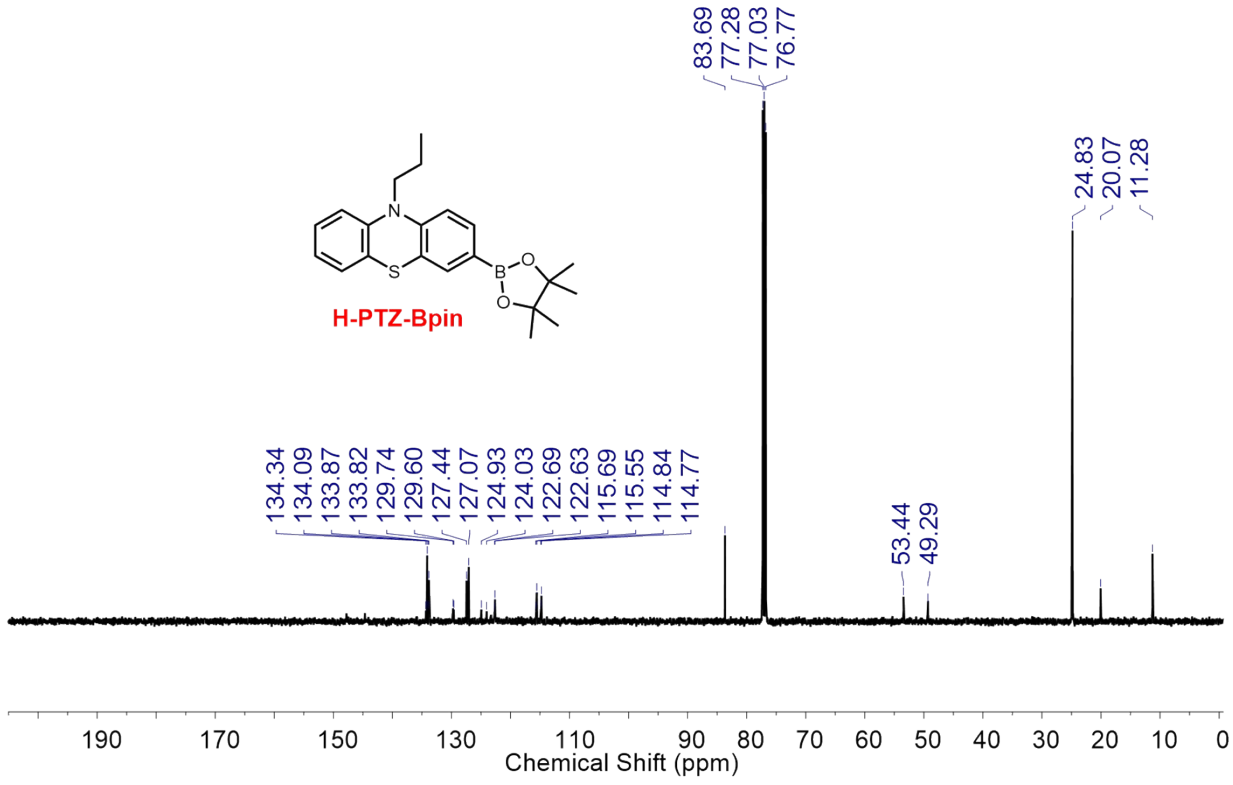

Figure S2. $^{13}C\{^{1}H\}$ NMR of **H-PTZ-Bpin** ($CDCl_3$, 126 MHz).

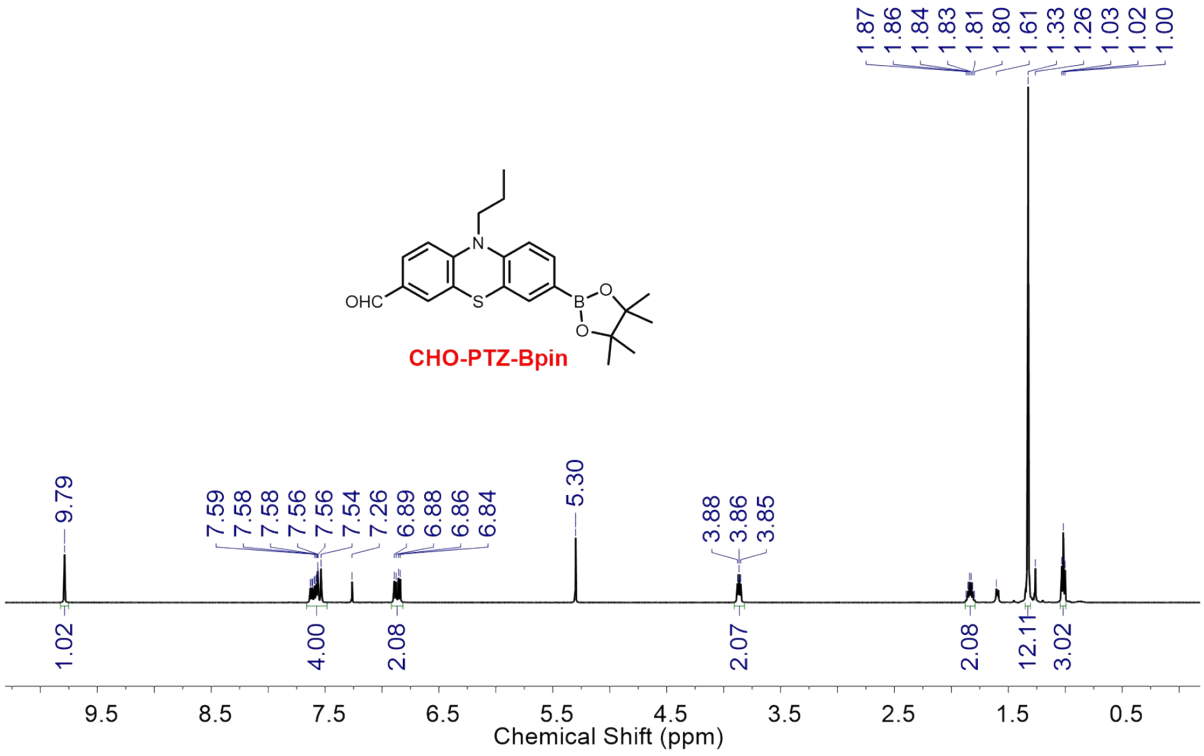

Figure S3. ^{1}H NMR of **CHO-PTZ-Bpin** ($CDCl_3$, 500 MHz).

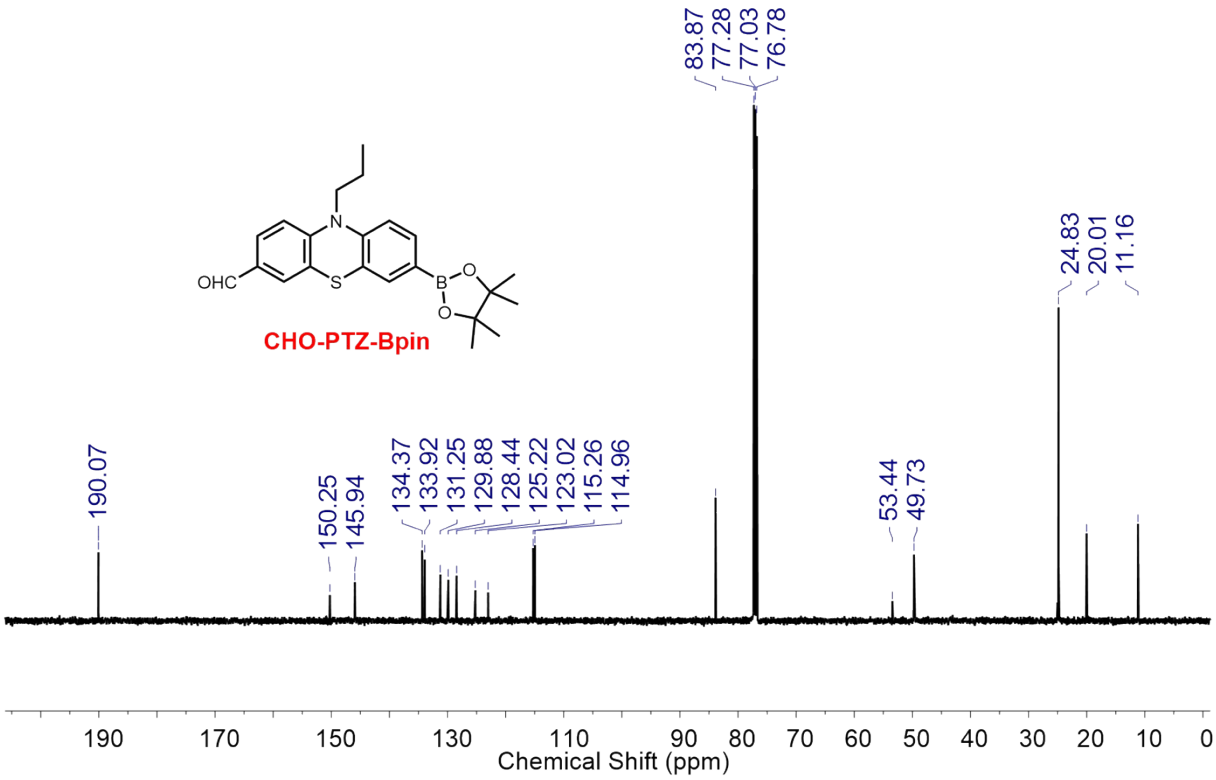

Figure S4. $^{13}C\{^{1}H\}$ NMR of **CHO-PTZ-Bpin** ($CDCl_3$, 126 MHz).

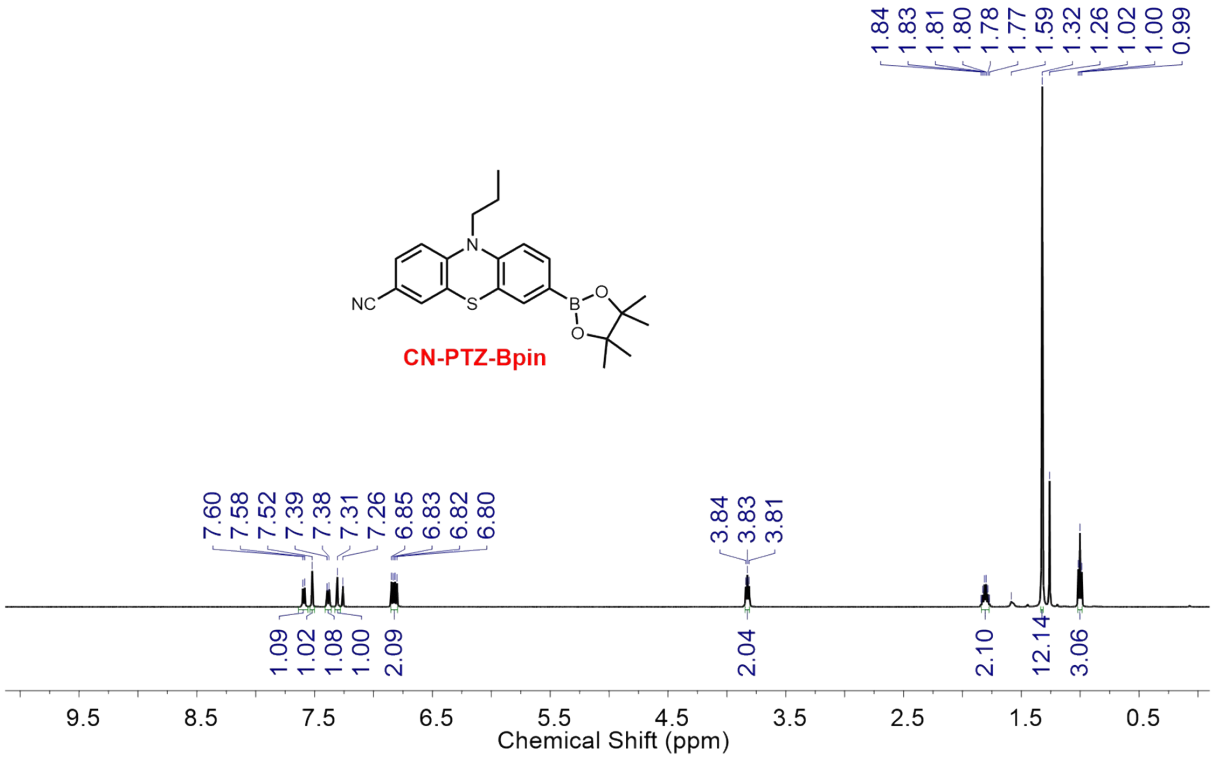

Figure S5. ^{1}H NMR of **CN-PTZ-Bpin** ($CDCl_3$, 500 MHz).

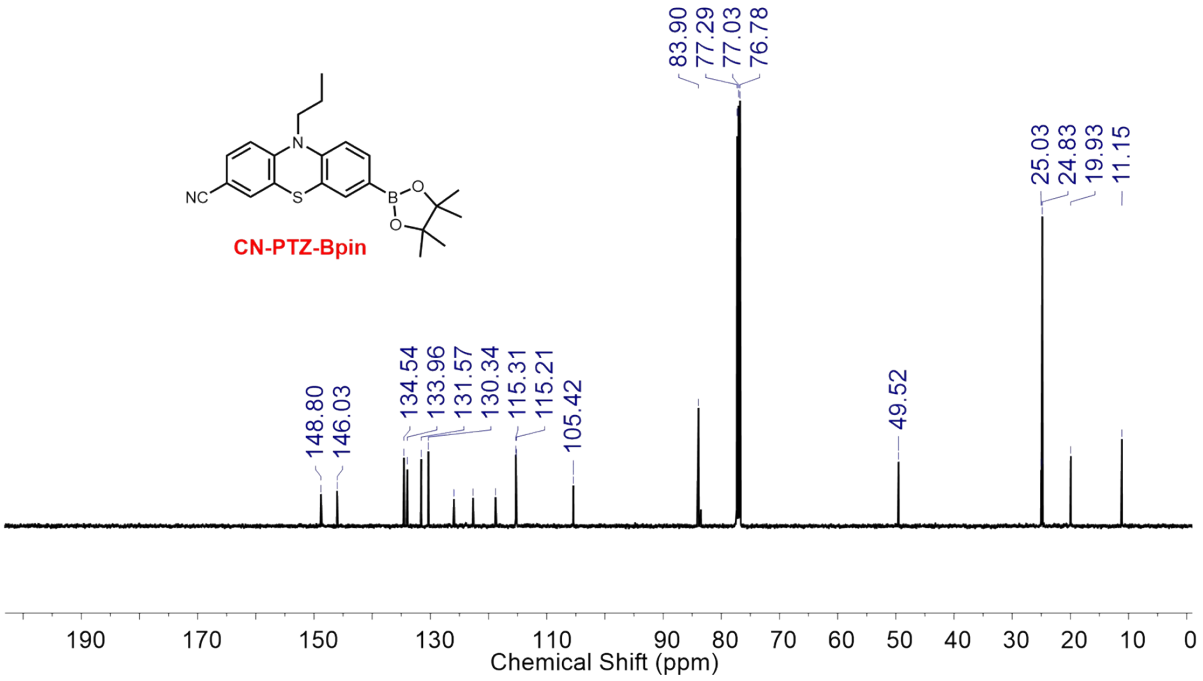

Figure S6. ^{13}C{^{1}H} NMR of **CN-PTZ-Bpin** ($CDCl_3$, 126 MHz).

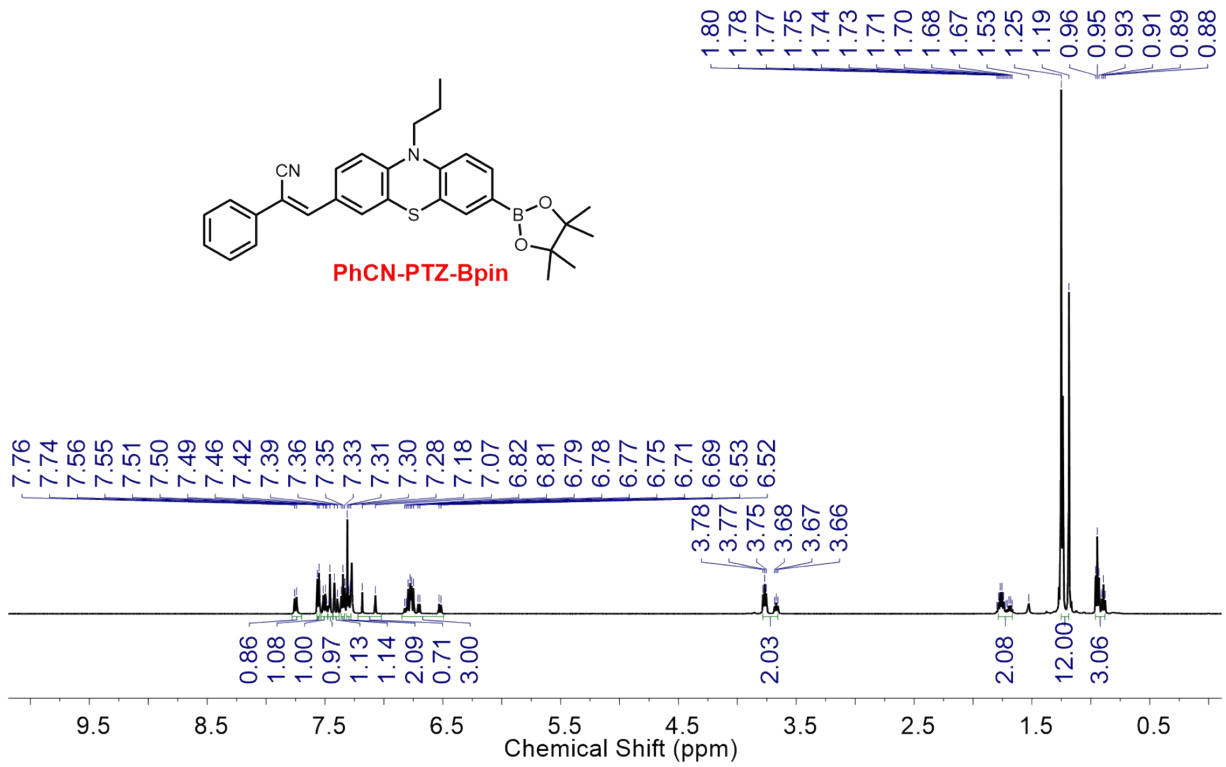

Figure S7. ^{1}H NMR of **PhCN-PTZ-Bpin** ($CDCl_3$, 500 MHz).

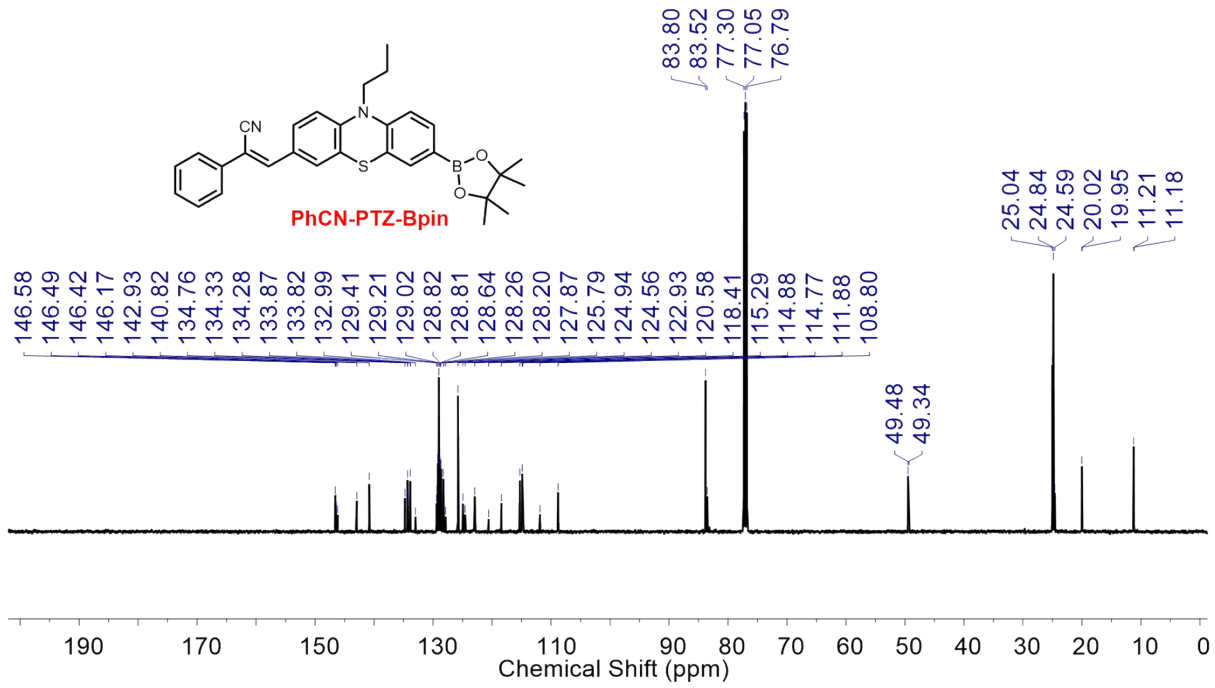

Figure S8. $^{13}C\{^{1}H\}$ NMR of **PhCN-PTZ-Bpin** ($CDCl_3$, 126 MHz).

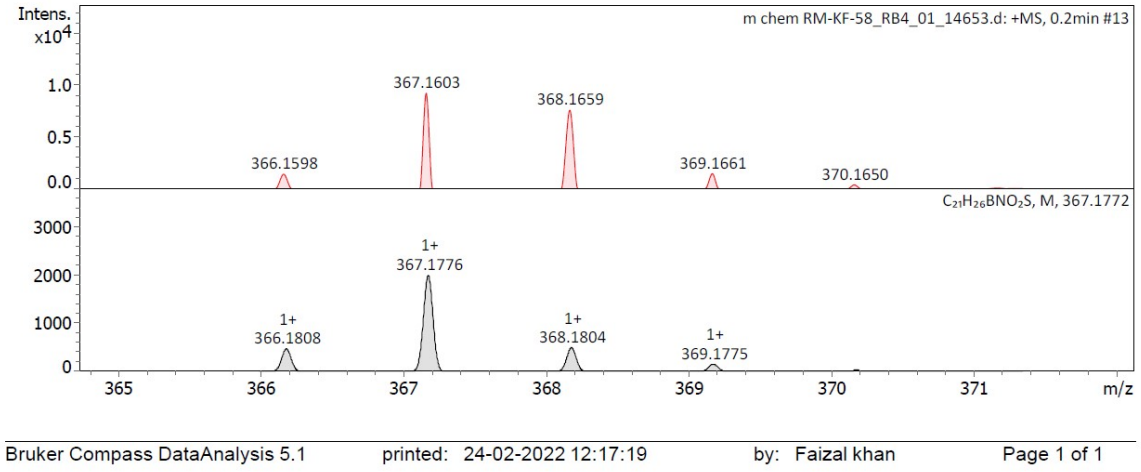

Figure 9. HRMS of **H-PTZ-Bpin**.

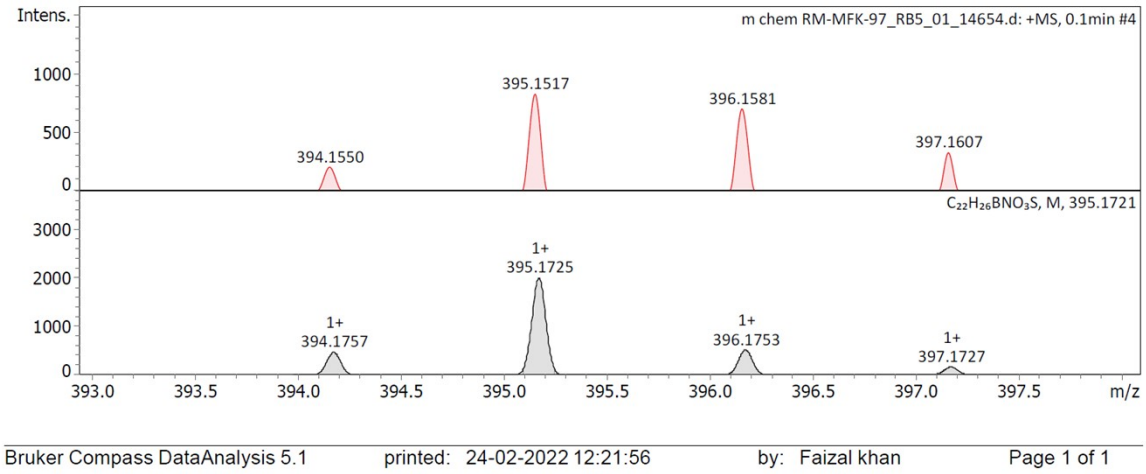

Figure 10. HRMS of **CHO-PTZ-Bpin**.

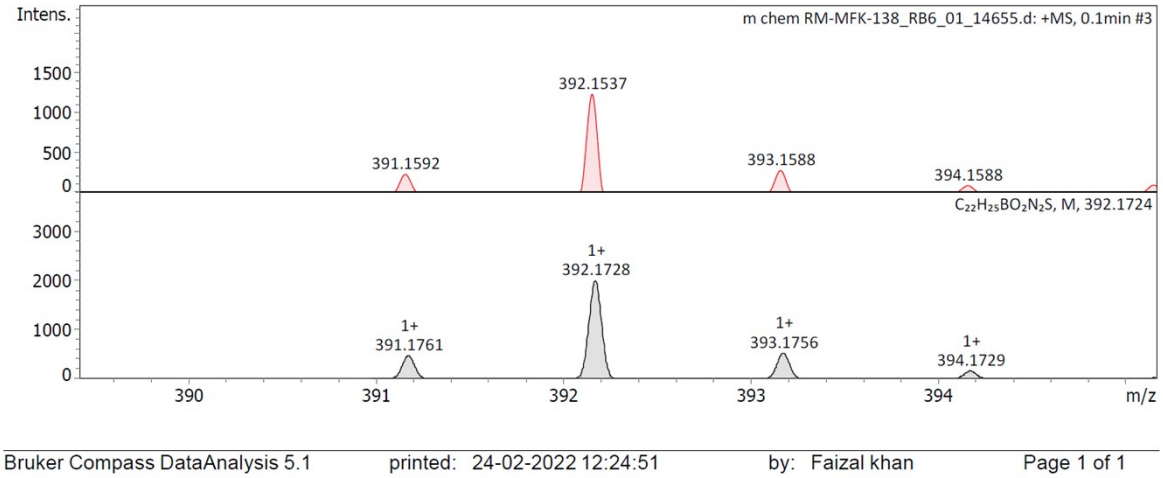

Figure 11. HRMS of **CN-PTZ-Bpin**.

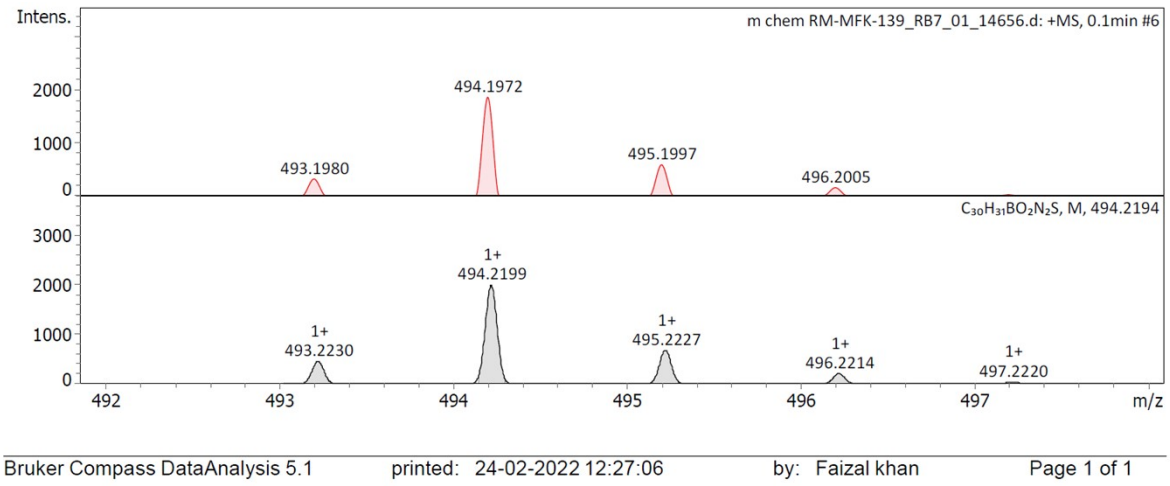

Figure 12. HRMS of **PhCN-PTZ-Bpin**.

Crystallographic data

The crystal and refinement data are summarized in Table S. The CCDC number 2176341 contains the supplementary crystallographic data for **CN-PTZ-Bpin**. These data can be obtained free of charge via www.ccdc.cam.ac.uk (or from the Cambridge Crystallographic Data Centre, 12 union Road, Cambridge CB21 EZ, UK; Fax: (+44) 1223- 336-033; or deposit@ccdc.cam.ac.uk). The efficient CH···O, S···π and CH···HC interactions were observed between the adjacent molecules which led to the formation of a supramolecular network. The O-atom of boronic ester group in each **CN-PTZ-Bpin** molecule interact with the H-atom of alkyl group of its neighbouring molecule through the CH···O interactions (2.679 Å) which leads to the formation of 1D ordered arrangement of **CN-PTZ-Bpin** (Figure S13a, Figure S14a and c). Similarly, The S-atom of phenothiazine in each **CN-PTZ-Bpin** molecule show S···π interactions with the aromatic ring of phenothiazine moiety of its neighbouring molecule forming a slipped stack of **CN-PTZ-Bpin** molecules (Figure 13b, Figure S14b and d). These 1D chains were further linked together by various CH···HC (2.399 Å) intermolecular interactions forming a supramolecular network of **CN-PTZ-Bpin** (Figure 13c, Figure S15). As a result of these strong intermolecular interactions, a stable lattice environment could be established for **CN-PTZ-Bpin**.

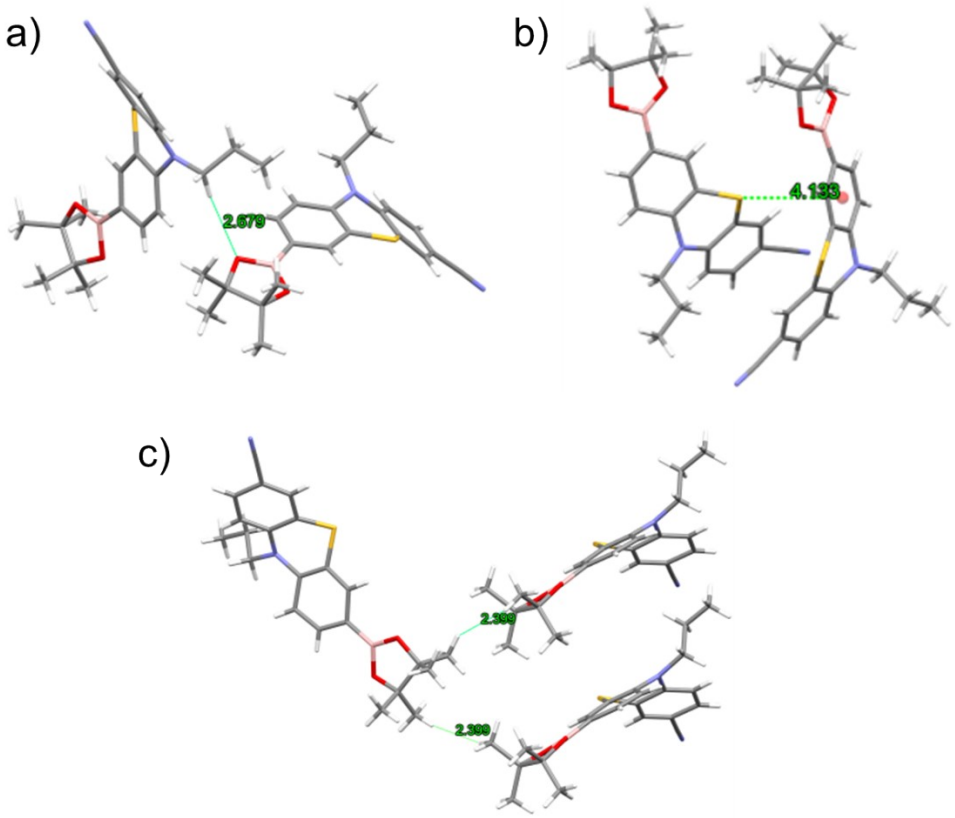

Figure S13. Single crystal structure of **CN-PTZ-Bpin** showing intermolecular interactions (a) CH···O, (b) S···π and (c) CH···HC.

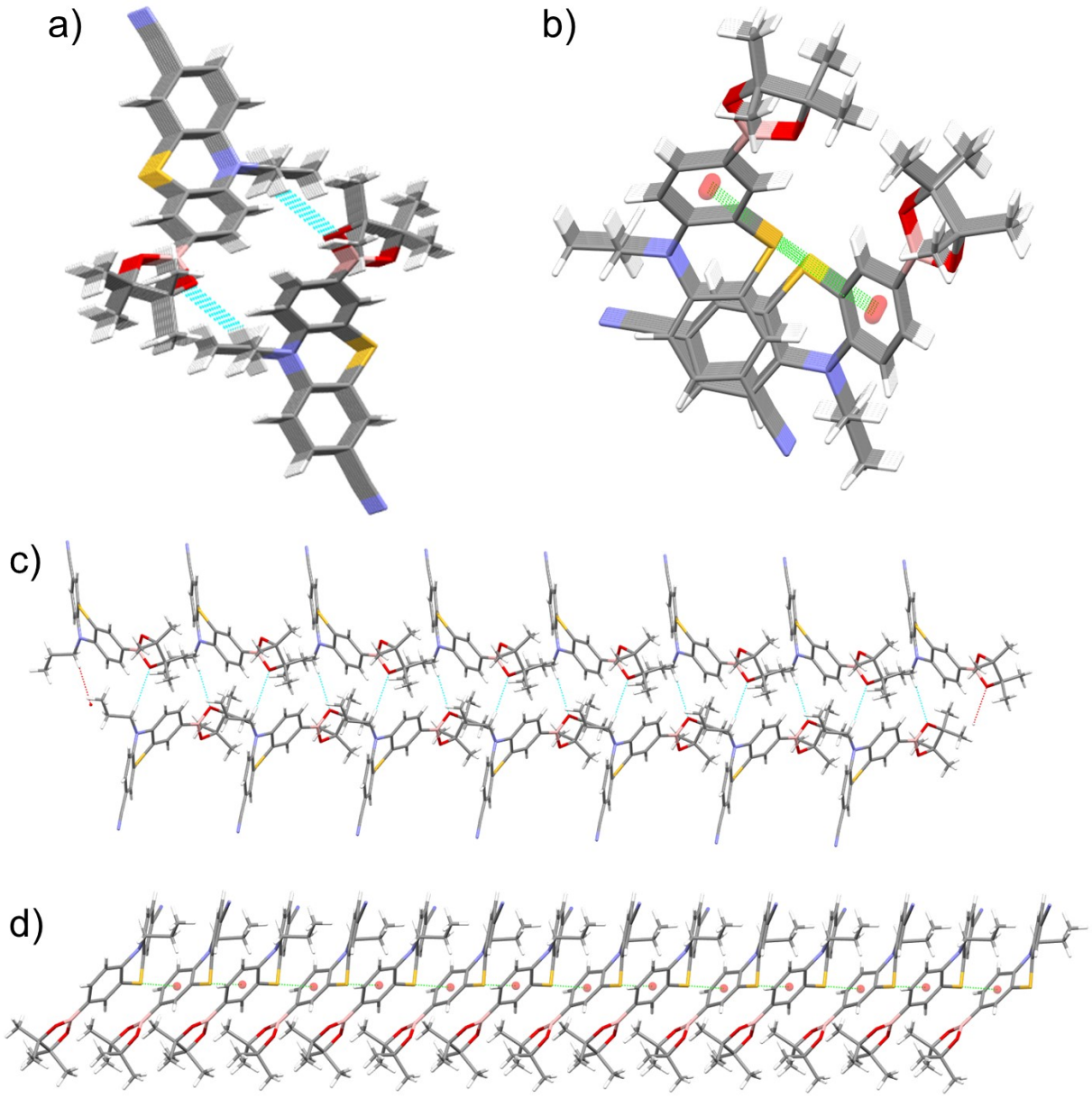

Figure S14. (a and c) 1D-arrangement of of the molecules of **CN-PTZ-Bpin** interacting through CH···O interactions (2.658 Å); (b and d) A slipped stacked arrangement of of the molecules of **CN-PTZ-Bpin** showing S···π interactions.

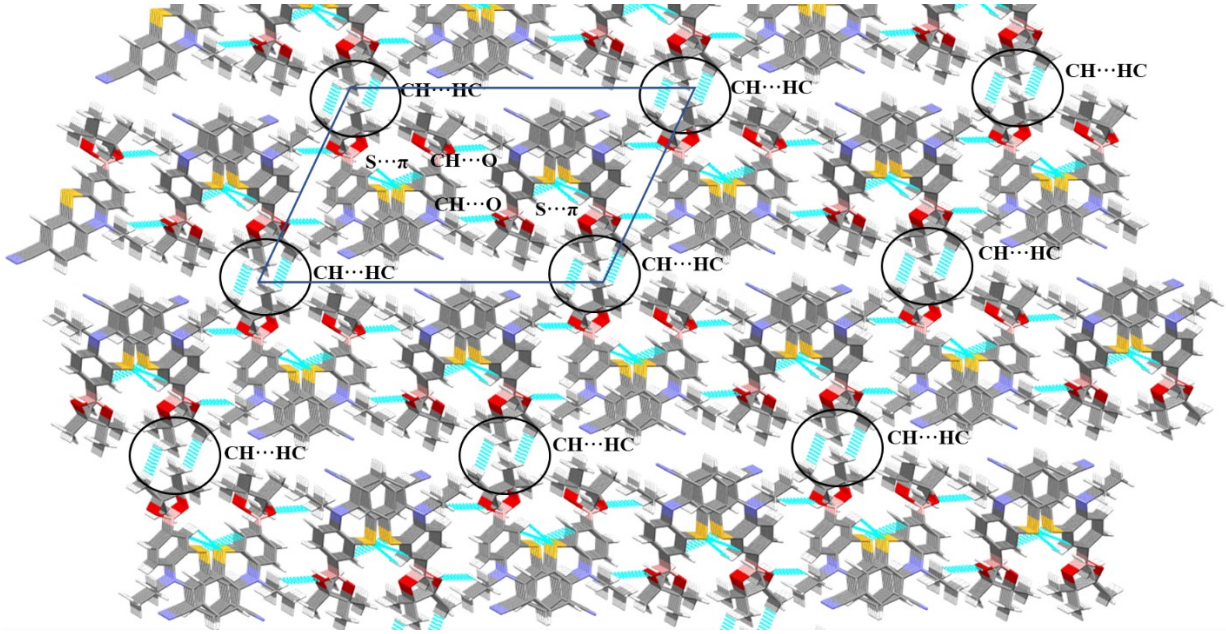

Figure S15. Supramolecular network of the molecules of **CN-PTZ-Bpin** in its crystalline lattice showing various intermolecular interactions.

Table S1 Crystal data and structure refinement for **CN-PTZ-Bpin**.

Identification code	**Rm669a**
Empirical formula	$C_{22}H_{25}BN_2O_2S$
Formula weight	392.31
Temperature	293(2)K
Wavelength	0.71073
Crystal system, space group	monoclinic, $P\text{-}2_1$
a/(Å)	13.914
b/(Å)	8.045
c/(Å)	20.630
Alpha/(°)	90.00
Beta/(°)	99.42
Gamma/(°)	90.00
Volume	2278.1(11) A^3
Z, calculated density	4, 1.144 g/cm^3
Absorption coefficient	0.160 mm^{-1}
F(000)	832.0
Crystal size	0.33 x 0.26 x 0.21
Θ range for data collection/(º)	6.356 to 58.804
Reflections collected	20439
Independent reflections	9886 [R_{int} = 0.2214, R_{sigma} = 0.4008]
Goodness-of-fit on F^2	0.905
Final R indexes [I>=2sigma(I)]	R_1 = 0.1133, wR2 = 0.2362

Final R indexes [all data]	R_1 = 0.3913, wR2 = 0.3623

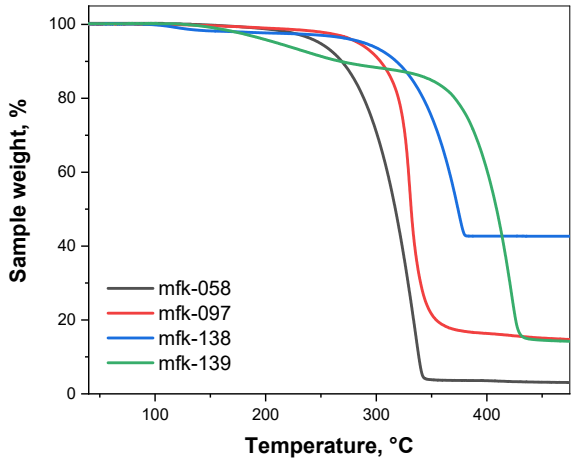

Figure S16. TGA curves of compounds **H-PTZ-Bpin**, **CHO-PTZ-Bpin**, **CN-PTZ-Bpin**, and **PhCN-PTZ-Bpin**.

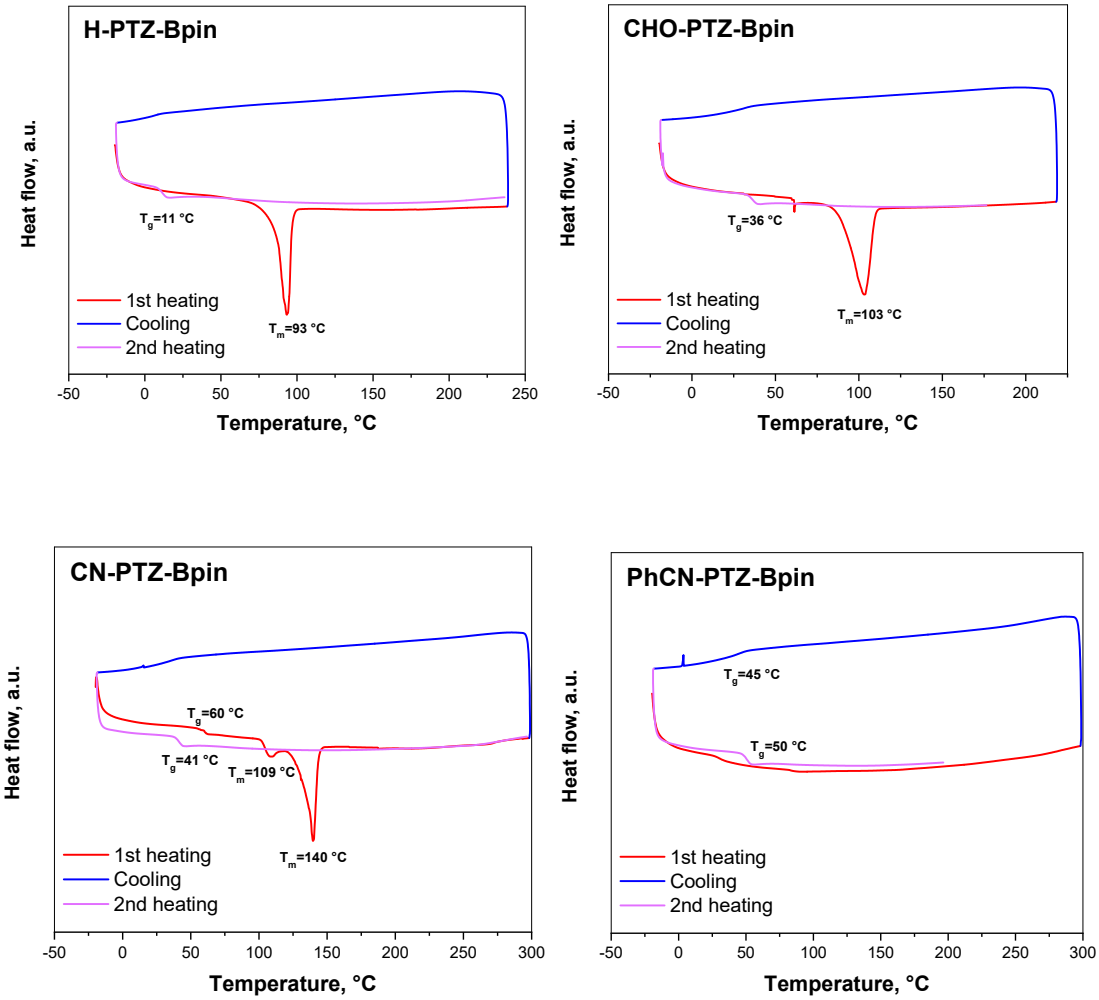

Figure S17. DSC curves of compounds **H-PTZ-Bpin**, **CHO-PTZ-Bpin**, **CN-PTZ-Bpin**, and **PhCN-PTZ-Bpin**.

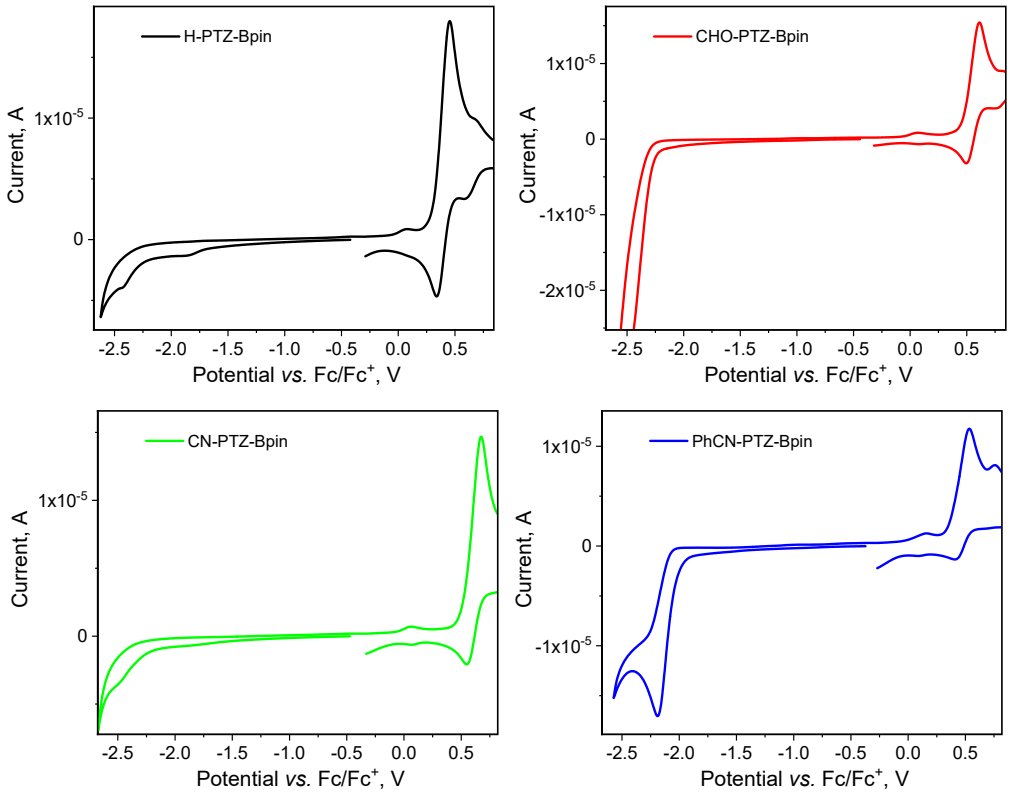

Figure S18. Cyclic voltammograms of compounds **H-PTZ-Bpin**, **CHO-PTZ-Bpin**, **CN-PTZ-Bpin**, and **PhCN-PTZ-Bpin**.

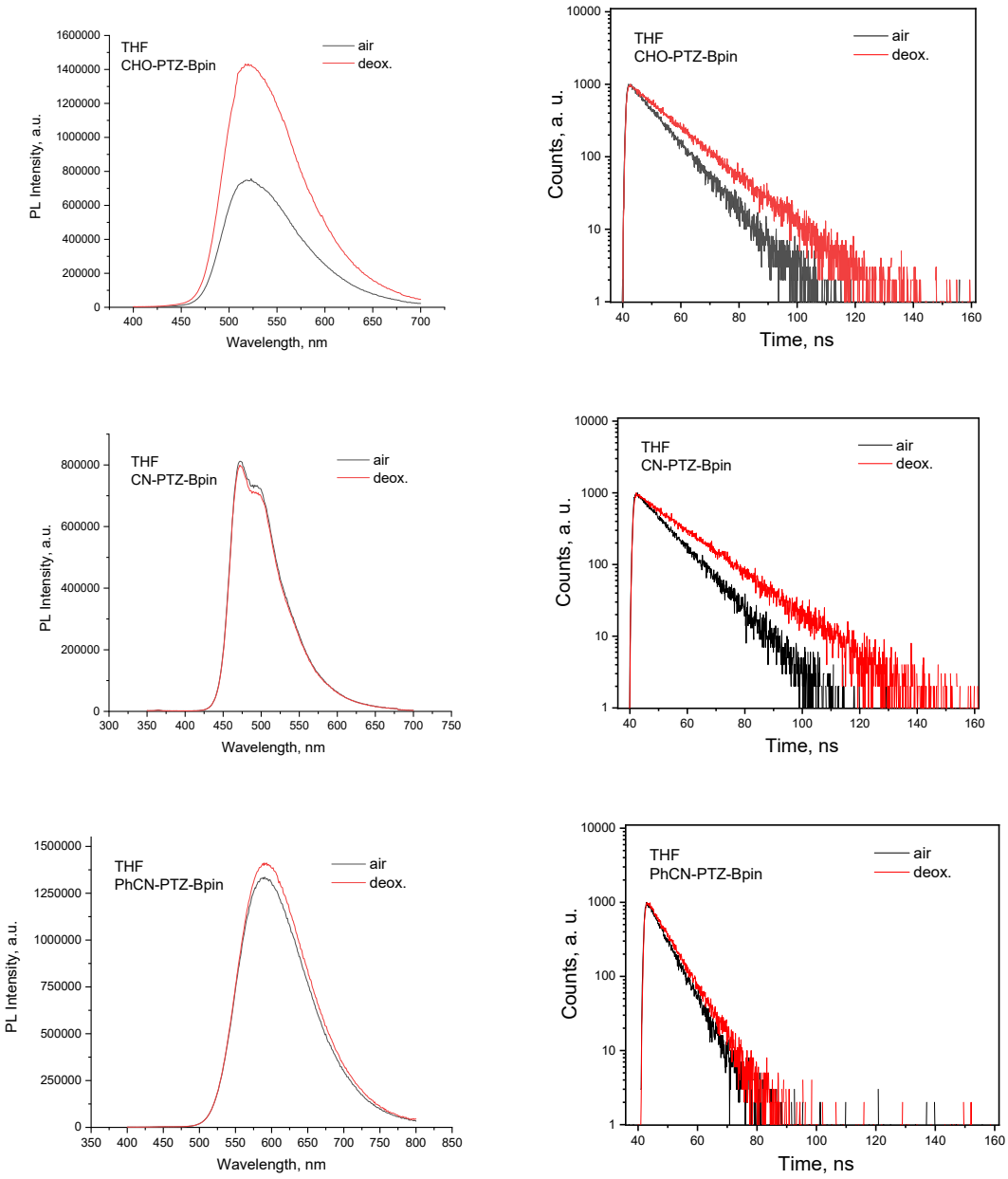

Figure S19. PL spectra (left) and PL decay curves (right) of non-deoxygenated (air) and deoxygenated (deox.) THF solutions of **CHO-PTZ-Bpin**, **CN-PTZ-Bpin**, and **PhCN-PTZ-Bpin** at room temperature.

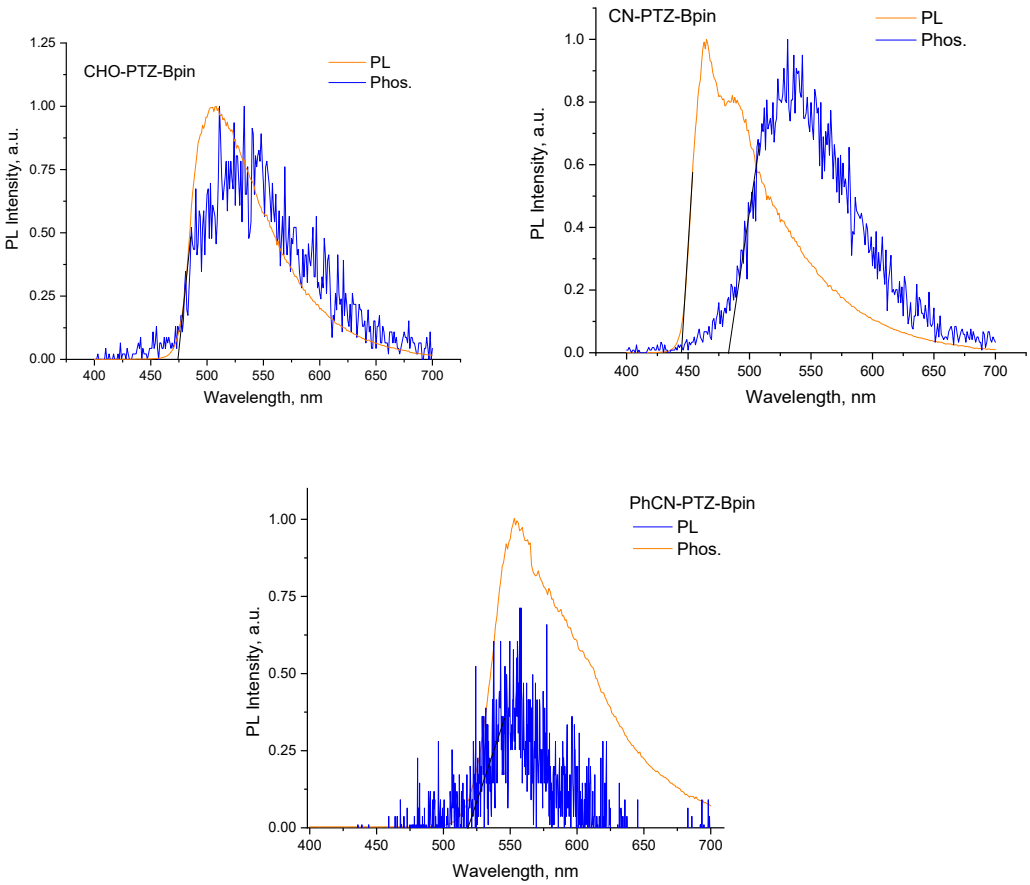

Figure S20. PL and phosphorescence spectra of **CHO-PTZ-Bpin**, **CN-PTZ-Bpin**, and **PhCN-PTZ-Bpin** in THF at 77K. Phosphorescence was separated from fluorescence using a delay of 1ms after excitation.

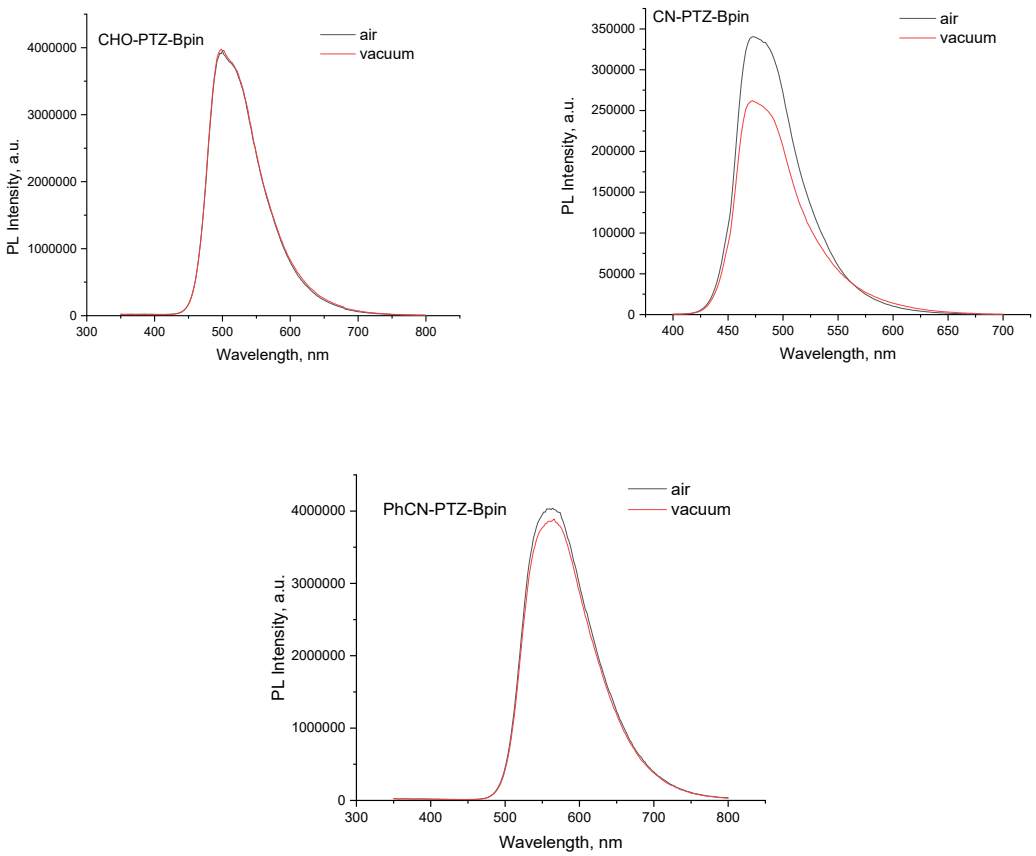

Figure S21. PL spectra of low-concentrated (5 wt.%) dispersions of **CHO-PTZ-Bpin**, **CN-PTZ-Bpin**, and **PhCN-PTZ-Bpin** in ZEONEX under air and vacuum at room temperature.